Revised application of copper ion selective electrode (Cu-ISE) in marine waters: a new meta-calibration approach

Saša Marcinek[a,*], Arnaud Chapoulie[b], Pascal Salaün[c], Scott Smith[d], Dario Omanović[a,*]

[a]Ruđer Bošković Institute, Center for Marine and Environmental Research, Bijenička cesta 54, 10000 Zagreb, Croatia
[b]Ecole Nationale Supérieure d'Ingénieurs de Caen (ENSICAEN), 6 Boulevard Maréchal Juin, 14050 Caen, France
[c]Department of Earth and Ocean Sciences, University of Liverpool, Liverpool L69 3GP, UK
[d]Department of Chemistry and Biochemistry, Wilfrid Laurier University, 75 University Avenue West, Waterloo, ON, N2L 3C5, Canada

Corresponding authors: smarcin@irb.hr, omanovic@irb.hr

Abstract

Copper (Cu) is a bio-essential trace element that is of concerns due to its potential toxicity at concentrations commonly encountered in coastal waters. Here, we revisit the applicability of Cu(II) ion selective electrode (Cu-ISE) based on a jalpaite membrane for the measurement of Cu_{free} in seawater. At high total Cu concentration (> 0.1 mM), (near)Nernstian slope was obtained and determination of Cu_{free} down to fM levels was possible. However, this slope decreases with decreasing total Cu concentration (e.g. 7 mV/decade at 15 nM total Cu) making the use of a common single calibration approach unreliable. To solve this problem, we carried out several calibrations at different levels of total Cu (15 nM - 1 mM) and ethylenediamine (EN: 5 µM - 15 mM) and fitted the calibration parameters (slope and intercept) as a function of total Cu using the Gompertz function (a meta-calibration approach). The derived empirical equations allowed the determination of Cu_{free} at any total Cu concentration above 20 nM (determination of Cu_{free} at lower total Cu levels is prevented by the dissolution of the electrode). We successfully tested this meta-calibration approach in UV digested seawater in presence of a synthetic ligand (EN), isolated natural organic matter (humic acid, HA) and in a natural estuarine sample. In each case, our meta-calibration approach provided a good agreement with modeled speciation data (Visual MINTEQ), while standard single approach failed. We provide here a new method for the direct determination of the free Cu ion concentration in seawater at levels relevant for coastal waters.

Keywords: copper ion selective electrode, meta-calibration, speciation, trace metals

1. Introduction

Copper (Cu) is an essential micronutrient required in a number of cellular processes that are key to phytoplankton growth [1-4], It is also a well-known toxic element to phytoplankton and other living organisms and in most cases, the Cu_{free} metal ion is the bioavailable specie [5], although this is not always the case [6]. In algal cultures, Cu_{free} concentrations as low as 10 pM and 100 pM were found toxic to cyanobacteria and dinoflagellates, respectively [7]. These Cu toxicity thresholds are dependent on the species, the strains and the environment they live in [8, 9] but they are relatively low. Cu toxicity has been observed in waters impacted by atmospheric deposition [10-12], or in coastal waters [13, 14]. For accurate assessment of its potential toxicity to biota, the knowledge of the free ion concentration, which is considered as the key indicator [15, 16], is needed. In aqueous systems, Cu is present at nM levels but is extensively complexed to natural organic ligands, strongly reducing its free ion concentration [17, 18]. Presence of organic ligands is therefore of main significance in assessing Cu bioavailability [19-22].

Determination of the Cu_{free} ion concentration is thus challenging due to its low total concentration and extensive complexation by organic ligands. There is currently no simple, direct and sufficiently sensitive method to measure routinely [Cu_{free}] in marine systems. Determination cannot be achieved by standard dynamic techniques based on flux-based measurements (e.g. anodic stripping voltammetry ASV, diffusive gradients in thin-film gels DGT) because of the dissociation of labile compounds in the diffusion layer [23]. Free metal ion concentration can be estimated using equilibrium based methods such as CLE-CSV (Competitive Ligand Exchange – Cathodic Stripping Voltammetry) [24, 25], anodic stripping voltammetry (ASV) in equilibrium conditions [26], PLM (permeation liquid membrane) [27], ion-exchange column [28] or using a selective adsorption onto a chelating resin followed by medium exchange [29] and finally, by using an ion selective electrode (ISE). A new promising electroanalytical technique for measurement of free metal ion concentration called "absence of gradients and Nernstian equilibrium stripping" (AGNES) [30, 31] was recently used for the determination of free Cu by using gold vibrating electrode [26]. Due to its complexity, it is still not widely applied. Ion selective electrodes (ISE) are specifically designed to be sensitive to the free metal ion and they present several significant advantages: simple application, portability, fast response, robustness and low cost. There is a large number of ISEs for various cations and anions and the most known example is a Cu-ISE [32] based on jalpaite membrane. This

electrode has a low detection limit enabling not only free Cu (Cu_{free}) determination in natural samples, but also total Cu (Cu_T; in acidified and UV treated samples, corrected for the known inorganic side reaction) and the Cu complexing capacity (CuCC) [33-41]. However, their application in marine waters still face several challenges. First, the alteration of the electrode surface upon continuous interaction with sample matrix (e.g. electrode corrosion, electrode fouling by the chloride, hydroxide, organic ligands or other interferences, or deposition of copper sulphide/silver chloride film on the electrode surface [32, 42, 43]) is resulting in a drift of the electrode response, which can be minimized by using a preconditioning step in a sample with similar matrix [32, 43]. Secondly, electrode dissolution (i.e. release of Cu from the electrode surface to the solution) restricts the analysis to solutions that have Cu_T below ~ 20 nM [44, 45]. Solutions to minimize this dissolution problem include a flow-through system [40, 46] or the use of a strong hydrodynamic flow via high stirring, decreasing Cu_T down 0.1 nM [45-47]. If Cu_T is high enough at the electrode surface (i.e. in excess of the Cu levels originating from the dissolution of the electrode), very low Cu_{free} concentrations can be measured (down to a reported 10^{-19} M) [32, 40, 48, 49].

Under the assumption that the electrode response is caused by the Cu ion concentration at the electrode surface, controlled by rapid and reversible reactions at the electrode-solution interface (which do not change the composition in the solution), potential of the electrode can be related to the Cu ion activity (or Cu^{2+} concentration at constant ionic strength) (Eq. 1) [40, 50-52]:

$$E = E^0 + S \times \log[\mathrm{Cu_{free}}] \quad (1)$$

where E is the measured electrode potential, S is the slope and E^0 the intercept or reference potential. Plotting E vs. log[Cu_{free}] should give a Nernstian slope of nominally 29.6 mV/decade change in Cu_{free} ion concentration.

The applicability of Cu-ISE in seawater has been tested in a number of studies which all concluded that if the electrode is calibrated in standard Cu_{free} buffer (e.g. Cu-EN solution), it can be used for Cu_{free} measurement in spite of a high chloride content [37, 43, 47, 53]. In this work, we re-examine the applicability of Cu-ISE (based on jalpaite membrane) for the measurement of Cu_{free} in seawater. Cu-ISE methodology is commonly based on the use of single calibration approach which consists in taking a solution with a similar matrix as the sample, adding a very high level of Cu (typically 0.2 – 1 mM), adding a Cu-ligand of known stability constant (typically ethylenediamine; EN) and varying

95 [Cu_{free}] by controlling the pH [37, 40, 46, 53]. We show here that this approach is flawed because
96 the Nernstian behavior predicted by Eq. 1 is not observed at lower [Cu_T] (15 nM - 100 µM). To
97 overcome this problem, we applied a meta-calibration approach i.e. set of calibrations at various
98 Cu_T (15 nM – 1 mM) using EN (5 µM - 15 mM) to buffer Cu_{free}. The set of calibration parameters
99 (slope and intercept) were then fitted using the Gompertz function, allowing the choice of
100 optimized values at any Cu_T concentration. Our new meta-calibration approach was tested in UV
101 digested seawater in presence and absence of organic ligands (EN or humic acid) and in a natural
102 estuarine sample) for the determination of complexing parameters (ligand concentrations and
103 stability constants). For each of those tests, we compared the two approaches (single and meta-
104 calibration) to predictions from a modelling software Visual MINTEQ [54]. To our knowledge, this
105 is the first time that a meta-calibration approach is used for speciation of Cu using Cu-ISE.
106
107 **2. Material and methods**
108 All measuring solutions were prepared using ultrapure water (18.2 MΩ, Synthesis, Millipore, USA;
109 referred thereafter as Milli-Q). Copper stock solutions were prepared by appropriate dilutions of
110 an atomic absorption spectrometry standard solution (1 g dm^{-3}, pH = 2; *TraceCERT*, Fluka). pH
111 control was achieved by addition of a borate buffer containing 1 M boric acid (H_3BO_3; *Suprapur*,
112 Sigma-Aldrich) and 0.6 M sodium hydroxide (NaOH; *suprapur*, Merck). Acidification and
113 neutralization were obtained via addition of dilute hydrochloric acid (HCl; *suprapur*, Merck) or
114 sodium hydroxide (NaOH; *suprapur*, Merck). Ethylenediamine (EN) (puriss. p.a., ≥99.5%, Sigma-
115 Aldrich) stock solutions were prepared at concentrations of 1 and 10 mM. A humic acid stock
116 solution (HA; 600-1000 Da, Sigma-Aldrich), was prepared by dissolution in 1 mM NaOH. Prepared
117 solution of 2 mg dm^{-3} HA contains ~ 1 mg dm^{-3} dissolved organic carbon (DOC). Experiments were
118 performed in synthetic solutions using sodium nitrate or sodium chloride (both *suprapur*, Merck)
119 to regulate the ionic strength, or in organic matter free seawater (UVSW). UVSW was UV-oxidized
120 using a homebuilt system (250 W high-pressure mercury vapor lamp), for 24 h to decompose
121 natural organic matter; it was then purified using MnO_2 suspension for 24 h at room temperature
122 before filtration through pre-cleaned 0.22 µm CA filters (Sartorius) [55].

123 The free ion copper concentration was determined using an Orion Cu-ISE (Model 9429BN) having
124 a jalpaite $Ag_{1.5}Cu_{0.5}S$ membrane. Potentials were recorded relative to a double junction

Ag|AgCl|sat. NaCl reference electrode (model 6.0728.120+6.1245.010, Metrohm, Switzerland) containing purified UVSW as the outer filling solution in the bridge. The pH was simultaneously recorded during each experiment using a double junction pH electrode calibrated against NIST (*National Institute of Standards and Technology*) traceable pH buffer solutions (Merck). Each electrode was connected to a dedicated potentiometer (Orion research, Expandable ion Analyzer EA 920). The voltage outputs of both potentiometers were connected to the high-resolution data acquisition USB datalogger ADC-20 (Pico Technology, Cambridge, UK) which was used to convert analog signal to digital form. A homebuilt software was developed for data collection/recording, graphical presentation and treatment.

If not used for longer period, the sensor membrane (jalpaite) was protected with the plastic cover cap provided by the producer. After prolonged period of continuous use (~ 1 week), storage (>1 month) or decrease of the electrode response, the electrode is polished by using the polishing kit supplied by the producer. Between measurements, the Cu-ISE was stored in slightly acidified Milli-Q water (pH ~ 5) in the dark, because it was shown that storage in darkness minimizes the undesirable photooxidation of the $Ag_{1.5}Cu_{0.5}S$ membrane [47, 56]. Before the measurements, it was rinsed with Milli-Q water and conditioned for at least one hour in an identical solution as the one to be measured, until a steady potential value had been obtained. All measurements were made in 20 mL solutions, at room temperature (~ 24 °C) under constant stirring (magnetic stirrer, 950 rpm). Solutions for electrode calibration were prepared in 4 different media (0.1 and 0.5 M NaCl, UVSW and 0.5 M $NaNO_3$) at various Cu_T concentrations (1 mM – 15 nM) in presence of EN. Concentration of EN at each Cu_T concentration was chosen to maintain $[Cu_{free}]$ below 0.1 pM ($\log[Cu_{free}] < -13$) at the highest pH value. For the electrode calibrations, the Cu_{free} concentration in the solution was varied by adjusting the pH. At the beginning of the acid titration, pH of the solution was set above 8.5 using borate buffer (0.02 M) and gradual additions of the dilute HCl solution were used to lower the pH down to ~ 3 (there is no complexation of Cu by EN at this low pH, only inorganic complexation occur) [43]. The cell potential was recorded upon stabilization after each acid addition, using a stability criterion of 0.15 mV min^{-1}. The electrode slopes (potential vs $\log[Cu_{free}]$) were calculated by linear regression and were reproducible to within ±2.4 mV/decade over a one-year period.

Equilibrium speciation calculations of Cu_{free} were performed using Visual MINTEQ (*MINeral Thermal EQuilibrium model*) [54]. Cu_T and EN concentrations were corrected for the dilution factor due to the addition of acid. This was done automatically by Visual MINTEQ using a prepared Excel file. A seawater composition of salinity 38 (Table S1) was used to setup Visual MINTEQ in order to calculate Cu_{free} needed in experiments performed in UVSW. The modeling of Cu interaction with model humic acid (HA) organic matter was performed by using default setup provided in Visual MINTEQ. For modeling of natural organic matter representing estuarine sample, a default model setup comprising 100% fulvic acid (FA) was used.

Cu titrations (addition of an increasing concentration of Cu_T) were performed in: (1) model solutions (0.5 M $NaNO_3$, 0.1 and 0.5 M NaCl and UVSW) without organic ligands at pH 3 and 8.5; (2) model solutions (0.5 M NaCl and UVSW) with addition of EN or HA as organic Cu-ligands and (3) in a natural estuarine water sample (collected in the Krka River estuary, Croatia, in July 2019 (GPS coordinates: 43°44'07.92 N, 15°52'39.61 E) at 0.5 m depth, *S* = 28). The latter sample was filtered through 0.22 µm CA filters (Sartorius) by using pre-cleaned syringe (5% v/v HNO_3, rinsed 3 times with Milli-Q water) and stored at 4 °C in pre-cleaned (1% v/v HCl, rinsed 3 times with Milli-Q water) FEP (Nalgene) bottle until analysis. Total dissolved Cu was measured by means of standard addition method using differential pulse anodic stripping voltammetry (DPASV) in an acidified (pH 2) UV digested sample [57]. Measurements were carried out using an PGSTAT128N potentiostat (Metrohm-Autolab, Utrecht, The Netherlands) controlled by GPES 4.9 software in a three-electrode cell (663 VA Stand, Metrohm). DOC concentration was determined by high temperature catalytic oxidation using a Shimadzu TOC-VCSN carbon analyzer [58]. Cu titrations were performed by increasing the Cu concentration with 11-15 additions equally distributed in logarithmic scale, i.e. similar increments in $\log[Cu]_T$ [17, 59]. The potential was measured by Cu-ISE after every Cu addition and converted to Cu_{free} by both the single and the new proposed meta-calibration approaches. By plotting the dependance of Cu_{free} on increasing Cu_T concentrations, the titration curves were constructed. Treatment of the titration curve obtained in natural estuarine sample was performed using the ProMCC software which provided an estimation of complexation parameters (concentration of Cu-complexing ligands [L_i] and conditional stability constants; K'_{CuLi}) [60].

3. Results and discussion

3.1. Standard single Cu-ISE calibrations

Calibration curves (Fig. 1) of electrode potential vs log[Cu_{free}] obtained in 0.5 M $NaNO_3$, 0.1 M NaCl, 0.5 M NaCl or UVSW in presence of a high concentration of copper (300 μM Cu_T) and 1 mM EN had regression lines with (near)Nernstian slopes of 30.2, 29.7, 27.7 and 24.9 mV/decade, respectively. However, while the linearity in 0.5 M $NaNO_3$ and 0.1 M NaCl was good along the entire range (-13 < log[Cu_T] < -3) with R^2 of 0.9989 and 0.9999, good linearity in UVSW and 0.5 M NaCl was only obtained when [Cu_{free}] < ~ 1 μM. At higher concentrations, the pH is such that Cu-buffering by EN is low and chloride interference occurs [61]. Chloride interference was already observed, at [Cu_{free}] > 10^{-8} M, due to a formation of Cu(I)-chloro complexes in the electrode diffusion layer at high [Cu_{free}] [50, 56, 61]. However, for [Cu_{free}] < ~ 1 μM, (near)Nernstian slopes were also obtained (28.8 and 27.1 mV/decade for 0.5 NaCl and UVSW respectively). These slopes are in agreement with those reported in the literature (Table 1).

We repeated these calibration curves in the same solutions but with a lower Cu_T concentration of 300 nM. Linear relationships were still obtained but the slopes of the regression lines (Table 1) were all significantly lower (21.6, 14.8 and 12.5 mV/decade in 0.5 M $NaNO_3$, 0.5 M NaCl and UVSW respectively). Decrease of slopes between high and low Cu_T was more pronounced in chloride containing solutions (47% and 52% loss in 0.5 NaCl and UVSW respectively) than in chloride free solution (28% loss in 0.5 M $NaNO_3$). These results are generally consistent with those found by Avdeef et al. (1983) [48] who reported a 10% decrease of slope in 10 mM KNO_3 when passing from 1 mM Cu_T down to 200 nM Cu_T.

It thus appears that the electrode response is dependent on the total Cu concentration. To test this hypothesis, we carried out meta-calibrations at different Cu_T concentrations.

3.2. Cu-ISE meta-calibrations

To estimate the dependence of the Cu-ISE calibration parameters on [Cu_T], calibrations were performed at various concentrations of Cu_T (in the range 1 mM – 15 nM) and EN (15 mM - 5 μM) in UVSW (Fig. 2), 0.5 M NaCl (Fig. S1) and 0.5 M $NaNO_3$ (Fig. S2). All calibrations produced linear response down to pM/fM level of Cu_{free} and slopes (mV per decade of Cu_{free}) were found to decrease with decreasing Cu_T.

Calibration parameters (i.e. slope, S and the reference potential, E^0) at a given Cu_T were calculated by fitting all the experimental points. They are shown against log[Cu_T] in bottom graphs of Figs. 2, S1 and S2. The regression slopes decreased from a (near)Nernstian values (at Cu_T above ~ 50 µM) down to 7.3 and 9.4 mV/decade in UVSW and 0.5 M NaCl (at 15 nM Cu_T), respectively and down to 21.9 mV/decade in 0.5 M $NaNO_3$ (at 35 nM Cu_T); the intercept decreased from 234 mV to 45 mV in UVSW, 264 mV to 85 mV in 0.5 M NaCl and 323 mV to 255 mV in 0.5 M $NaNO_3$ (at referred Cu_T concentrations).

Both calibration parameters followed a sigmoidal relationship with Cu_T, the greatest variation being between 35 nM and 10 µM Cu_T ($-7.0 < \log[Cu_T] < -5.0$) in all three media (Figs. 2, S2 and S3). At high Cu levels (Cu_T above ~ 50 µM), both S and E^0 were relatively constant. With decreasing concentrations, S decreased showing a loss of sensitivity towards Cu_{free}. The lowest reachable potential at Cu_T below 0.3 µM was ~ -60 mV while, for the same log[Cu_{free}], potential was ~-120 mV at Cu_T > 10 µM. At Cu_T below 20 nM, S and E^0 both reach a constant value, irrespective of Cu_T. This is due to the dissolution of the electrode membrane which sets up the detection limit of the ISE [45].

Several attempts have been made to explain the chloride interference on Cu-ISE measurements: some of them considered the exchange reactions at the electrode surface and other redox reactions with membrane material [52, 56, 61, 62]. Lewenstam et al. (1985) [52] provided a model which describes how the presence of halide ions affects the exchange reactions at the electrode-solution interface by forming amorphous sulphur. According to these authors, this reaction mechanically blocks the electrode surface and causes irreversible reactions, which may be the explanation of the more prominent loss of sensitivity towards Cu_{free} in the high chloride media observed here.

Whatever the reasons, we can conclude that this significant change of calibration parameters (S and E^0) at varying Cu_T concentration simply prevents the use of a single calibration approach. For reliable measurements, potentials have to be correlated to the appropriate calibration curve, which is dependent on the Cu_T concentration. To predict the correct S and E^0 at any [Cu_T], we tried to fit experimental results on various sigmoidal functions, among which the Gompertz function (Eq. 2) showed the best matching:

$$f(x) = y_0 + ae^{-e^{\frac{(x-x0)}{b}}} \quad (2)$$

where y_0 is the base value, x_0 is the Cu_T at mid-slope value, while a and b are fitting parameters, not having any chemical meaning. The fitted equations for S and E^0 in UVSW are given in Fig. 2 (see Fig. S1 for 0.5 M NaCl). Note that "S"-shaped Gompertz function is used here due to the wide range of the examined Cu_T. However, if the calibrations are performed in the narrower range of Cu_T (e.g. up to 10 µM), the obtained relationships might not be fully sigmoidal, and as such, the other empirical functions could also be used (e.g. polynomial or other sigmoidal functions), as long as the fitting of the datasets is satisfactory.

The proposed meta-calibration approach for determination of Cu_{free} concentration comprises the two prerequisites: (1) the known concentration of Cu_T in the sample being analyzed and (2) the two valid Gompertz (or other) functions needed to create calibration line (slope + intercept) at any concentration of Cu_T (they are electrode dependent). For measurements at lower Cu_T concentrations (~ <1 µM), it is suggested that the electrode is conditioned by the sample being analyzed for at least 30 minutes, after which the new fresh sample is taken, and the potential reading taken upon stabilization.

Based on the results presented above, we suggest the following analytical protocol for the determination of Cu_{free} in chloride containing media:

1. determine the Gompertz functions for both the slope and intercept; ideally, this should be obtained in the expected range of Cu_T and at salinity close to the sample of interest,
2. determine the dissolved Cu_T concentrations of the samples of interest,
3. measure the potential (E) using Cu-ISE electrode,
4. determine the Cu_{free} concentration based on equation (1) using the appropriate calibration parameters (S and E^0) extracted by using the Gompertz functions (step 1) for the known concentration of dissolved Cu_T (step 2).

3.3. Applicability of the meta-calibration approach

3.3.1. Model solution without organic ligands

The response of the electrode was first tested in absence of organic ligands at pH of 3 and 8.5 for each of the following solution: 0.5 M $NaNO_3$, UVSW, 0.1 and 0.5 M NaCl. Cu levels were increased

from 15 nM to 110 µM and [Cu_{free}] were obtained from Visual MINTEQ predictions. At pH 3, the expected theoretical slope was again obtained in 0.5 M $NaNO_3$ and 0.1 M NaCl (28.9 and 29.5 mV/log[Cu_{free}], respectively), whereas a "super-Nernstian" response was obtained in UVSW and 0.5 M NaCl at pH 3 (38.0 and 41.3 mV/log[Cu_{free}], respectively), and at pH 8.5 (38.1 and 38.3 mV/decade, respectively) (Figs. 3, 4 and S3). All experiments were repeated several times over a period of one year and they gave similar results. At pH 3, the electrode response to Cu_T additions in UVSW and 0.5 M NaCl was linear down to ~ 25 nM Cu_{free}, whereas it was linear down to ~ 1 nM Cu_{free} at pH 8.5 (Figs. 4A/B and S3A/B) as a result of buffering effect of carbonate and hydroxide present in the solution (Table S2). This is consistent with the previous observation that, in the absence of any organic ligand, buffering effect of hydroxy and carbonate complexes is enough to allow reliable measurements of Cu_{free} < 20 nM [49]. In the absence of organic ligands (Figs. 4A/B and S3A/B), the proportionality between Cu_T and Cu_{free} is given by the inorganic side reaction coefficient, α ([Cu_T]/[Cu_{free}]) [62]. At pH 3, $\alpha \sim 1.5$ due to Cu complexation with chloride and sulfate while at pH 8.5, $\alpha \sim 33$ due to complexation with carbonate and hydroxide. The observed shifts between [Cu_{free}] and [Cu_T] along the X-axis in Figs. 4A/B correspond to α-factors at two pH values.

The applicability of our meta-calibration approach was first checked in UVSW at both pH 3 (Fig. 4C) and 8.5 (Fig. 4D) by plotting Cu_{free} as a function of Cu_T using the single calibration approach (Fig. 1), the meta-calibration approach (i.e. using the empirical equations given in Fig. 2) or Visual MINTEQ predictions. Similar graphs are shown in Fig. S3C/D for 0.5 M NaCl. At both pH, the single calibration approach displayed a sigmoidal shape similar to what is usually obtained in the presence of organic ligands in solution: a weak curvature at the lowest Cu levels followed by a linear increase in Cu_{free} in response to higher Cu additions, analogous to ligand saturation. This response has been previously reported and explained by the lack of sensitivity of the Cu-ISE at the initial concentration level [37, 53]. However, when applying our meta-calibration approach, our calculated Cu_{free} concentrations are in much better agreement with modeled data than the single calibration approach. This is particularly true at pH 3. At pH 8.5, at Cu_T concentration above 10 µM, Cu precipitation of Cu hydroxide species is predicted, which may explain the plateau observed at these high Cu levels (top empty circles).

Super-Nernstian response to increasing Cu concentration was already observed in other studies and attributed to the presence of chloride ions [52, 62]. Using a Orion Cu-ISE, Jasinski et al. (1974) [62] observed a Nernstian slope in nitrate and sulfate media and a super-Nernstian slope in 1 M KCl at pH 2 and in 0.5 M NaCl at pH 8. They suggested that this anomalous response was due to both the electrode material and the high chloride ion concentration rather than the presence of small quantities of chelating agents in the solution. Belli and Zirino (1993) [53] reported super-Nernstian response in high-chloride media, but only in alkaline conditions. They assumed that the matrix binds different fraction of Cu, depending on the Cu concentration, in artificial seawater at pH 8 and that there are neglected Cu species in the model. We obtained slightly different slopes at pH 8.5 (Fig. 4) between E vs log[Cu_T] (slope of 38.8 mV/decade) and E vs log[Cu_{free}] (38.1 mV/decade) as a result of slight change in inorganic side reaction coefficient at increasing Cu concentration, mostly coming from hydroxide ions. Notwithstanding, this difference is quite negligible and is probably not the reason for super Nernstian response during Cu titration, as suggested by Belli and Zirino (1993) [53]. Moreover, the same response was also observed here at pH 3 where the inorganic side reaction coefficient is constant. Super-Nernstian response most likely occurs due to the gradual shift in sensitivity during increasing Cu_T concentration. Finally, if we take only the two last points from the Cu titration at pH = 3 (Fig. 4A), where [Cu_T] is high enough (Fig. 2), we obtain a Nernstian slope of 28.89 mV/-log[Cu].

The decrease of slope with lowering Cu_T concentration might explain the strong disagreement of experimental results with the predicted ones in the presence of synthetic ligands (EN and the polyaminocarboxylic acids EDTA, CDTA and NTA) at lower Cu_T concentration (< 1 µM) obtained by Rivera-Duarte and Zirino (2004) [37], which was also specifically pointed out by Sánchez-Marín (2020) [39]. The leveling of pCu they observed below 10 nM of Cu_T is related to the detection limit of Cu-ISE electrode caused by the dissolution of the electrode membrane, maintaining the relatively high Cu_T in the vicinity of the electrode surface [45]. Furthermore, in their experiment in the absence of organic matter (Fig. 2 in [37]), a disagreement between modeled and measured [Cu_{free}] are in agreement with our results when using the single calibration approach (Fig. 4C/D). As shown here in Fig. 4C/D, using proposed meta-calibration approach the agreement with modeled data for the same experiment type was much better, signifying the benefit of our calibration approach for the measurements of Cu speciation in natural waters.

330 *3.3.2. Model solutions with known concentrations of organic ligands*

331 The validity of our meta-calibration approach was also tested in UVSW (pH = 8.2) in presence of
332 organic ligands, either 5 μM EN or 2 mg dm^{-3} HA. Cu titrations were achieved in both solutions and
333 concentrations of Cu_{free} were calculated at each step using the single and meta-calibration
334 approaches and compared to Visual MINTEQ predictions (Fig. 5).

335 In both cases, the meta-calibration approach provided a much better agreement with the modeled
336 values that the single calibration approach. In presence of EN (Fig. 5A/B), both methods displayed
337 a good agreement with Visual MINTEQ at Cu_T levels above 10 μM (because of similar calibration
338 parameters in these conditions; Fig. 2) but the single calibration approach significantly
339 overestimated Cu_{free} at Cu_T levels below ~ 1 μM. In presence of HA, the single calibration approach
340 strongly underestimated Cu_{free} at higher Cu levels and strongly overestimated them at lower. At Cu
341 levels below ~ 30 nM ($\log[Cu_T] < -7.5$), a plateau value limit was reached confirming that Cu-ISE is
342 not suitable for measurements of lower levels in our cell configuration. This would prevent the
343 analysis of open ocean or open coastal seas that contain low nM levels of Cu [63], but it can allow
344 Cu speciation (i.e. measurements of Cu_T, Cu_{free} and Cu-binding organic ligands) in coastal areas with
345 strong anthropogenic influence [64].
346
347 *3.3.3. Natural estuarine sample*

348 The efficiency of the meta-calibration method in the determination of $[Cu_{free}]$, as well as in the
349 determination of concentration and strength of natural organic ligands, was evaluated here by Cu
350 titration on an estuarine sample collected from the Krka River estuary (pH = 8.2); this sample had a
351 total Cu concentration of 20 nM and contained 1.5 mg dm^{-3} DOC. Cu_{free} concentrations obtained
352 using the single and meta-calibration approaches, were compared to the modeled data obtained
353 by Visual MINTEQ (Fig. 6).

354 Very good agreement was obtained between the meta-calibration approach and Visual MINTEQ
355 predictions in the linear part of the titration curve (i.e. at $[Cu_T] > 3$ μM) while the single calibration
356 approach strongly underestimated $[Cu_{free}]$ in that region, similar to with HA (Fig. 5C/D). At the lower
357 end of $[Cu_T]$, the single calibration approach predicts a much higher $[Cu_{free}]$ (30 times higher, similar
358 to results obtained in presence of HA), whereas much closer values to those predicted by Visual

MINTEQ were obtained using meta-calibration approach. Although the general trend of measured [Cu_{free}] agree well with the predicted values along the full titration range, slightly higher values at the concentration range below 1 µM of Cu_T could be explained by the difference in the ligand characteristics of estuarine natural organic matter from the one used in Visual MINTEQ modeling (fulvic acid).

Ligand concentrations and conditional stability constants were calculated from each titration curve using ProMCC [60] and are compared in Fig. 7. Good agreement was obtained between Visual MINTEQ and the meta-calibration approach in terms of number of ligand classes (represented here as L_1, L_2 and L_3), their concentrations and associated stability constants. However, the strongest class of ligands L_1 was not identified when the single calibration approach was applied, which leads to ~ 50× overestimation of [Cu_{free}] calculated based on the derived complexation parameters (Fig. 7A). As this class of ligands ($\log K_1$) is the most important for the complexation of Cu at its low ambient concentration, the single calibration approach would therefore tend to highly overestimate the Cu toxicity of the sample.

4. Conclusions

This work demonstrates that at Cu_T concentrations below 100 µM, the Nernstian slope is decreasing with decreasing Cu_T for the jalpaite electrodes Although Cu concentrations can reach high levels in highly polluted coastal areas [19, 65, 66], they are almost never higher than 30 µM where effective calibration parameters begin to deviate from the theoretical values (Figs. 2 and S1). In natural waters, commonly occurring Cu_T concentrations are much lower and closer to the detection limit of Cu-ISE, preventing the use of the standard single calibration approach. We show here that a meta-calibration approach can be successfully used instead, by applying optimized calibration parameters at appropriate Cu_T level. The results obtained in synthetic solutions as well as in seawater are in good agreement with modeled predictions, preventing a high overestimation of Cu_{free} that is observed through the single calibration approach. This new analytical procedure is simple and could be used to enable Cu speciation studies in natural and synthetic samples, measurement of Cu_{free} in toxicological experiments and in a number of other studies. The sensitivity, the ease of use, the rapid response time and the robustness of the electrode over a long period of time are all assets to this new analytical procedure that can be used in natural waters,

389 including marine. The use of flow-through cell [40], rotating electrode [45] or highly efficient wall-
390 jet system [67] is expected to decrease the detection limit and/or associated problems of the
391 electrode dissolution. This is our next objective.
392
393 **Acknowledgment**
394 This research was realized within the scope of the project “New methodological approach to
395 biogeochemical studies of trace metal speciation in coastal aquatic ecosystems” (MEBTRACE),
396 financially supported by the Croatian Science Foundation under the project number IP-2014-09-
397 7530.
398
399 **References**
400 [1] D. Deruytter, M.B. Vandegehuchte, J. Garrevoet, F. De Laender, E. Vergucht, K. Delbeke, R. Blust, K.A.C.
401 De Schamphelaere, L. Vincze, C.R. Janssen, Environ. Toxicol. Chem., 34 (2015) 1330-1336.
402 [2] S.B. Goldhaber, Regulatory toxicology and pharmacology : RTP, 38 (2003) 232-242.
403 [3] G. Peers, N.M. Price, Nature, 441 (2006) 341-344.
404 [4] G. Peers, S.A. Quesnel, N.M. Price, Limnol. Oceanogr., 50 (2005) 1149-1158.
405 [5] P.G.C. Campbell, Interactions between trace metals and aquatic organisms: A critique of the free-ion
406 activity model, in: A. Tessier, D.R. Turner (Eds.) Trace Metal Speciation and Bioavailability in Aquatic Systems,
407 John Wiley & Sons, Chichester, 1995, pp. 45-102.
408 [6] P. Sanchez-Marin, E. Aierbe, J.I. Lorenzo, V.K. Mubiana, R. Beiras, R. Blust, Aquat. Toxicol., 178 (2016)
409 165-170.
410 [7] L.E. Brand, W.G. Sunda, R.R.L. Guillard, J. Exp. Mar. Biol. Ecol., 96 (1986) 225-250.
411 [8] P. Echeveste, P. Croot, P. von Dassow, Sci. Total Environ., 625 (2018) 1673-1680.
412 [9] R. Zitoun, S.J. Clearwater, C. Hassler, K.J. Thompson, A. Albert, S.G. Sander, Sci. Total Environ., 653 (2019)
413 300-314.
414 [10] A. Jordi, G. Basterretxea, A. Tovar-Sanchez, A. Alastuey, X. Querol, Proc Natl Acad Sci U S A, 109 (2012)
415 21246-21249.
416 [11] A. Paytan, K.R. Mackey, Y. Chen, I.D. Lima, S.C. Doney, N. Mahowald, R. Labiosa, A.F. Post, Proc Natl
417 Acad Sci U S A, 106 (2009) 4601-4605.
418 [12] T.J. Yang, Y. Chen, S.Q. Zhou, H.W. Li, Atmosphere, 10 (2019) 414.
419 [13] J. Karlsson, E. Ytreberg, B. Eklund, Environ. Pollut., 158 (2010) 681-687.
420 [14] E. Ytreberg, J. Karlsson, B. Eklund, Sci. Total Environ., 408 (2010) 2459-2466.
421 [15] G. Merrington, A. Peters, C.E. Schlekat, Environ. Toxicol. Chem., 35 (2016) 257-265.
422 [16] T.N. Tait, C.A. Cooper, J.C. McGeer, C.M. Wood, D.S. Smith, Environ Chem, 13 (2016) 496-506.
423 [17] Y. Louis, C. Garnier, V. Lenoble, S. Mounier, N. Cukrov, D. Omanović, I. Pižeta, Mar. Chem., 114 (2009)
424 110-119.
425 [18] K.N. Buck, J. Moffett, K.A. Barbeau, R.M. Bundy, Y. Kondo, J.F. Wu, Limnol Oceanogr-Meth, 10 (2012)
426 496-515.
427 [19] K.N. Buck, J.R.M. Ross, A.R. Flegal, K.W. Bruland, Environ. Res., 105 (2007) 5-19.
428 [20] M.I. Heller, P.L. Croot, Mar. Chem., 173 (2015) 253-268.
429 [21] J.W. Moffett, C. Dupont, Deep-Sea Res Pt I, 54 (2007) 586-595.

[22] Y. Louis, C. Garnier, V. Lenoble, D. Omanović, S. Mounier, I. Pižeta, Mar. Environ. Res., 67 (2009) 100-107.
[23] L. Sigg, F. Black, J. Buffle, J. Cao, R. Cleven, W. Davison, J. Galceran, P. Gunkel, E. Kalis, D. Kistler, M. Martin, S. Noel, Y. Nur, N. Odzak, J. Puy, W. Van Riemsdijk, E. Temminghoff, M.L. Tercier-Waeber, S. Toepperwien, R.M. Town, E. Unsworth, K.W. Warnken, L.P. Weng, H.B. Xue, H. Zhang, Environ. Sci. Technol., 40 (2006) 1934-1941.
[24] M.L.A.M. Campos, C.M.G. Van Den Berg, Anal. Chim. Acta, 284 (1994) 481-496.
[25] I. Pižeta, S.G. Sander, R.J.M. Hudson, D. Omanović, O. Baars, K.A. Barbeau, K.N. Buck, R.M. Bundy, G. Carrasco, P.L. Croot, C. Garnier, L.J.A. Gerringa, M. Gledhill, K. Hirose, Y. Kondo, L.M. Laglera, J. Nuester, M.J.A. Rijkenberg, S. Takeda, B.S. Twining, M. Wells, Mar. Chem., 173 (2015) 3-24.
[26] R.F. Domingos, S. Carreira, J. Galceran, P. Salaun, J.P. Pinheiro, Anal. Chim. Acta, 920 (2016) 29-36.
[27] N. Parthasarathy, J. Buffle, Anal. Chim. Acta, 284 (1994) 649-659.
[28] C. Fortin, Y. Couillard, B. Vigneault, P.G.C. Campbell, Aquat. Geochem., 16 (2010) 151-172.
[29] S. Noël, M.L. Tercier-Waeber, L. Lin, J. Buffle, O. Guenat, M. Koudelka-Hep, Electroanalysis, 18 (2006) 2061-2069.
[30] L.S. Rocha, J. Galceran, J. Puy, J.P. Pinheiro, Anal. Chem., 87 (2015) 6071-6078.
[31] J. Galceran, E. Companys, J. Puy, J. Cecilia, J.L. Garces, J. Electroanal. Chem., 566 (2004) 95-109.
[32] R. De Marco, G. Clarke, B. Pejcic, Electroanalysis, 19 (2007) 1987-2001.
[33] I.A.M. Ahmed, J. Hamilton-Taylor, S. Lofts, J.C.L. Meeussen, C. Lin, H. Zhang, W. Davison, Environ. Sci. Technol., 47 (2013) 1487-1495.
[34] J. Chen, H. Chen, X.W. Zhang, K. Lei, J.E. Kenny, Appl. Spectrosc., 69 (2015) 1293-1302.
[35] F. Delgadillo-Hinojosa, A. Zirino, C. Nasci, Mar. Environ. Res., 66 (2008) 404-411.
[36] T. Midorikawa, E. Tanoue, Y. Sugimura, Anal. Chem., 62 (1990) 1737-1746.
[37] I. Rivera-Duarte, A. Zirino, Environ. Sci. Technol., 38 (2004) 3139-3147.
[38] D.A. Roman, L. Rivera, Mar. Chem., 38 (1992) 165-184.
[39] P. Sánchez-Marín, Environ Chem, (2020).
[40] T.N. Tait, L.M. Rabson, R.L. Diamond, C.A. Cooper, J.C. McGeer, D.S. Smith, Environ Chem, 13 (2016) 140-148.
[41] H.B. Xue, W.G. Sunda, Environ. Sci. Technol., 31 (1997) 1902-1909.
[42] D.J. Crombie, G.J. Moody, J.D. Thomas, Talanta, 21 (1974) 1094-1098.
[43] R. De Marco, D.J. Mackey, A. Zirino, Electroanalysis, 9 (1997) 330-334.
[44] R.S. Eriksen, D.J. Mackey, R. van Dam, B. Nowak, Mar. Chem., 74 (2001) 99-113.
[45] A. Zirino, R. De Marco, I. Rivera, B. Pejcic, Electroanalysis, 14 (2002) 493-498.
[46] R.S. Eriksen, D.J. Mackey, P. Alexander, R. De Marco, X.D. Wang, J. Environ. Monit., 1 (1999) 483-487.
[47] A. Zirino, D.A. VanderWeele, S.L. Belli, R. DeMarco, D.J. Mackey, Mar. Chem., 61 (1998) 173-184.
[48] A. Avdeef, J. Zabronsky, H.H. Stuting, Anal. Chem., 55 (1983) 298-304.
[49] J. Rachou, C. Gagnon, S. Sauve, Environ Chem, 4 (2007) 90-97.
[50] B. Hoyer, Talanta, 38 (1991) 115-118.
[51] A. Hulanicki, A. Lewenstam, Talanta, 23 (1976) 661-665.
[52] A. Lewenstam, T. Sokalski, A. Hulanicki, Talanta, 32 (1985) 531-537.
[53] S.L. Belli, A. Zirino, Anal. Chem., 65 (1993) 2583-2589.
[54] J.P. Gustafsson, Visual MINTEQ ver. 3.1. https://vminteq.lwr.kth.se/, (2013).
[55] C.M.G. van den Berg, Anal. Chem., 78 (2006) 156-163.
[56] R. De Marco, Anal. Chem., 66 (1994) 3202-3207.
[57] A.M. Cindrić, C. Garnier, B. Oursel, I. Pižeta, D. Omanović, Mar. Pollut. Bull., 94 (2015) 199-216.
[58] S. Marcinek, C. Santinelli, A.M. Cindrić, V. Evangelista, M. Gonnelli, N. Layglon, S. Mounier, V. Lenoble, D. Omanović, Mar. Chem., 225 (2020) 103848.
[59] C. Garnier, I. Pižeta, S. Mounier, J.Y. Benaïm, M. Branica, Anal. Chim. Acta, 505 (2004) 263-275.
[60] D. Omanović, C. Gamier, I. Pižeta, Mar. Chem., 173 (2015) 25-39.

[61] J.C. Westall, F.M.M. Morel, D.N. Hume, Anal. Chem., 51 (1979) 1792-1798.
[62] Z.L. Zeng, N.W. Menzies, G. Kerven, Electroanalysis, 17 (2005) 912-914.
[63] S. Rodgher, A.T. Lombardi, G. Melao Mda, A.E. Tonietto, Ecotoxicology, 17 (2008) 826-833.
[64] R. Jasinski, I. Trachtenberg, D. Andrychuk, Anal. Chem., 46 (1974) 364-369.
[65] J.E. Jacquot, J.W. Moffett, Deep-Sea Res Pt Ii, 116 (2015) 187-207.
[66] A.C. Blake, D.B. Chadwick, A. Zirino, I. Rivera-Duarte, Estuaries, 27 (2004) 437-447.
[67] S.C. Apte, M.J. Gardner, J.E. Ravenscroft, Mar. Chem., 29 (1990) 63-75.
[68] J.R. Donat, K.A. Lao, K.W. Bruland, Anal. Chim. Acta, 284 (1994) 547-571.
[69] D. Omanović, Z. Peharec, T. Magjer, M. Lovrić, M. Branica, Electroanalysis, 6 (1994) 1029-1033.

Table 1. Composition of Cu activity buffers (Cu_{free} controlled by ligands) used for Cu-ISE calibration and derived calibration parameters (Eq. 1) – comparison with the literature data.

Solution	$[Cu_T]$ (M)	Ligand (M)	S (mV/decade)	E^0 (mV)	Electrode	Reference
0.5 M NaCl	$3e^{-4}$	EN; $1e^{-3}$	27.7	264	Orion	This study
*0.5 M NaCl	$3e^{-7}$	EN; $1e^{-5}$	14.8	146	Orion	This study
UVSW	$3e^{-4}$	EN; $1e^{-3}$	24.9	234	Orion	This study
*UVSW	$3e^{-7}$	EN; $1e^{-5}$	12.5	107	Orion	This study
0.1 M NaCl	$3e^{-4}$	EN; $1e^{-3}$	29.7	310	Orion	This study
0.5 M $NaNO_3$	$3e^{-4}$	EN; $1e^{-3}$	30.2	323	Orion	This study
*0.5 M $NaNO_3$	$3e^{-7}$	EN; $1e^{-5}$	21.6	261	Orion	This study
0.6 M NaCl	$1e^{-3}$	EN; $15e^{-3}$	30.7	273	Orion	Eriksen, et al. [46]
0.6M NaCl	$1e^{-3}$	EN; $15e^{-3}$	29.6	-	Orion	Tait, et al. [40]
ASW	$2e^{-4}$	Gly, EN; $1e^{-3}$	28	-	Orion	Belli and Zirino [53]
ASW	$2e^{-4}$	Gly, EN; $1e^{-3}$	27.6	-	Orion	Rivera-Duarte and Zirino [37]
0.01 M KNO_3	$1e^{-3}$	EN; $15e^{-3}$	29.4	308	Beckman	Avdeef, et al. [48]
*0.01 M KNO_3	$2e^{-7}$	EN; $15e^{-3}$	26.5	305	Beckman	Avdeef, et al. [48]
0.01 KNO_3	$1e^{-4}$	IDA; $1e^{-3}$	33	237	detecION	Rachou, et al. [49]
0.1 M $NaNO_3$	$1e^{-3}$	EN; $15e^{-3}$	28-30	320-327	Orion	Zeng, et al. [62]
0.1 M $NaNO_3$	$4.5e^{-4}$	NTA; $9e^{-4}$	29.4	306	ANALION	Rodgher, et al. [63]
0.1 M NaCl & 0.6 M NaCl	$2e^{-4}$	Gly; $1e^{-3}$	~30	-	Orion Radiometer	De Marco [56]
0.1 M NaCl & 0.6 M NaCl	$2e^{-4}$	Gly; $1e^{-3}$	29.5	-	Nafion-Orion	De Marco [56]
0.1 M NaCl & 0.6 M NaCl	$2e^{-4}$	Gly; $1e^{-3}$	20.9	-	Nafion-Radiometer	De Marco [56]

* Calibrations performed in solutions using low levels of Cu_T

Figure Captions

Figure 1. Electrode response to log[Cu_{free}] increase in 0.5 M $NaNO_3$, in 0.1 or 0.5 M NaCl and UVSW in presence of 0.3 mM Cu_T and 1 mM EN. Calibration lines are shown as dashed lines; slope values are expressed in mV/decade; log[Cu_{free}] was varied by adjusting the pH based on equilibrium speciation calculated by Visual MINTEQ.

Figure 2. Top: Electrode response to log[Cu_{free}] change in UVSW at various Cu_T concentrations. **Bottom:** Variation of the slope *S* (left graph) and intercept E^0 (right graph) vs log[Cu_T]. Data were fitted using the Gompertz equation (full lines); dashed lines represent 95% confidence interval.

Figure 3. Electrode response to Cu additions in 0.5 M $NaNO_3$, 0.1 and 0.5 M NaCl and UVSW at pH = 3. Regression lines are shown as dashed lines; slope values are expressed in mV/log[Cu_{free}]; [Cu_{free}] was calculated using Visual MINTEQ.

Figure 4. Top: Electrode response to log[Cu_T] (brown) and log[Cu_{free}] (green) change in UVSW at pH = 3 (A) and 8.5 (B). Regression lines are shown as dashed lines and points used for regression are indicated as full circles; equilibrium speciation was calculated using Visual MINTEQ. **Bottom:** Comparison between log[Cu_{free}] calculated using meta-calibration, standard single calibration (blue) and modeled using Visual MINTEQ (black) at pH = 3 (C) and 8.5 (D).

Figure 5. Complexometric titrations in UVSW comprising 5 µM EN (A, B) and 2 mg dm^{-3} HA (C, D): comparison between Cu_{free} concentrations calculated using meta-calibration approach (red), single calibration approach (blue) and modeled using Visual MINTEQ with (black) and without (white) organic ligands in the solution, in linear (A, C) and logarithmic scale (B, D). Insets: Corresponding *E*-log[Cu_T] curves.

Figure 6. Complexometric titration in a natural estuarine sample (the Krka River estuary, Croatia; sampled on July 2019) containing an initial [Cu_T] of 20 nM and 1.5 mg dm^{-3} DOC: Comparison is made between Cu_{free} concentration calculated using the meta-calibration approach (red), the single calibration approach (blue) and modeled using Visual MINTEQ with (black) and without (white) organic ligands in the solution, in linear (A) and logarithmic scale (B). Inset: Corresponding *E*-log[Cu_T] curves.

Figure 7. Comparison between Cu_{free} concentration and complexation parameters ([L_1], [L_2], [L_3], logK_1, logK_2 and logK_3) calculated from data obtained using meta-calibration, usual standard single calibration and modeled using Visual MINTEQ.

Figure 1

Click here to access/download;Figure;Figure_1.TIF

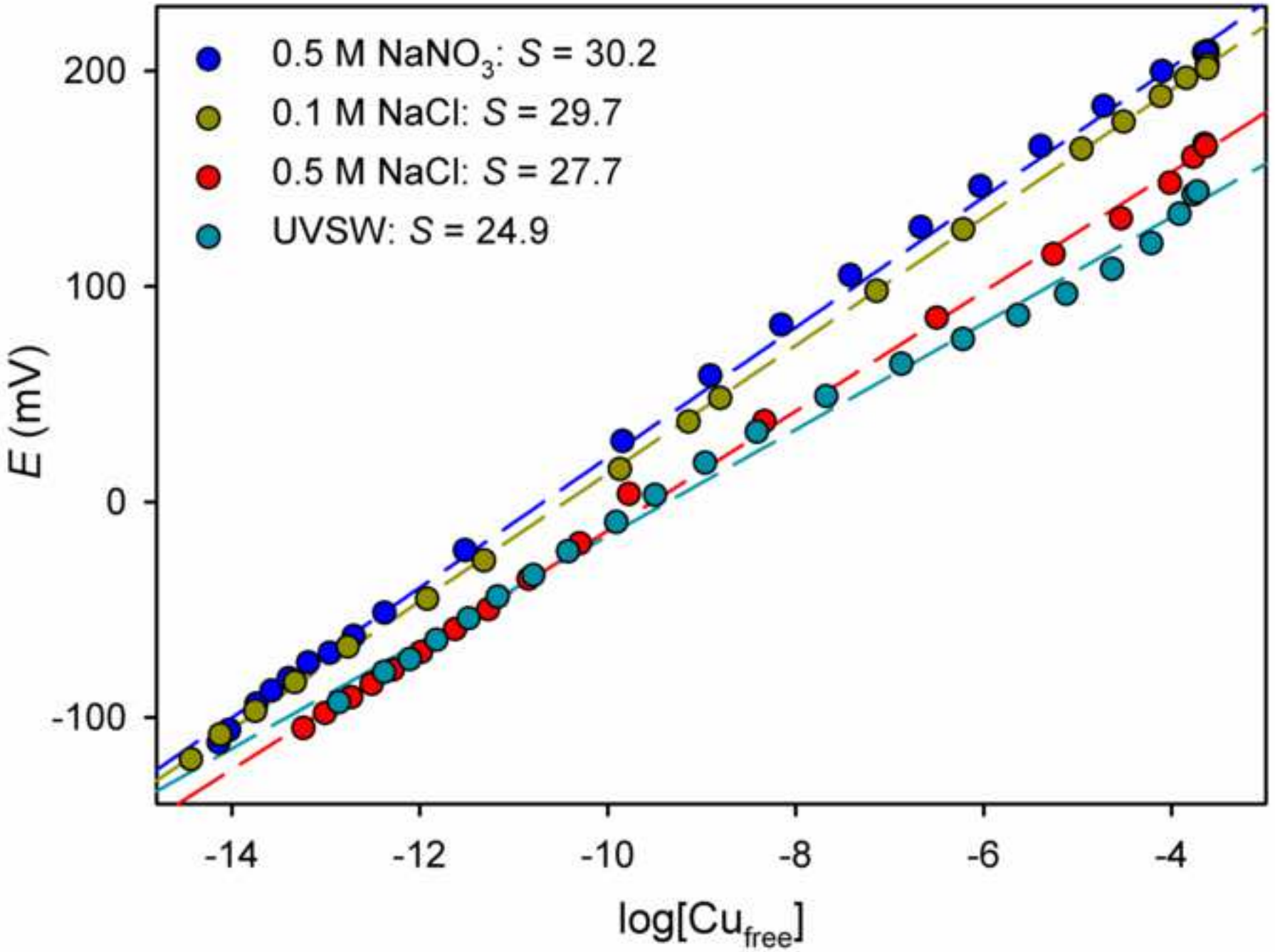

Figure 2

Click here to access/download;Figure;Figure_2.TIF

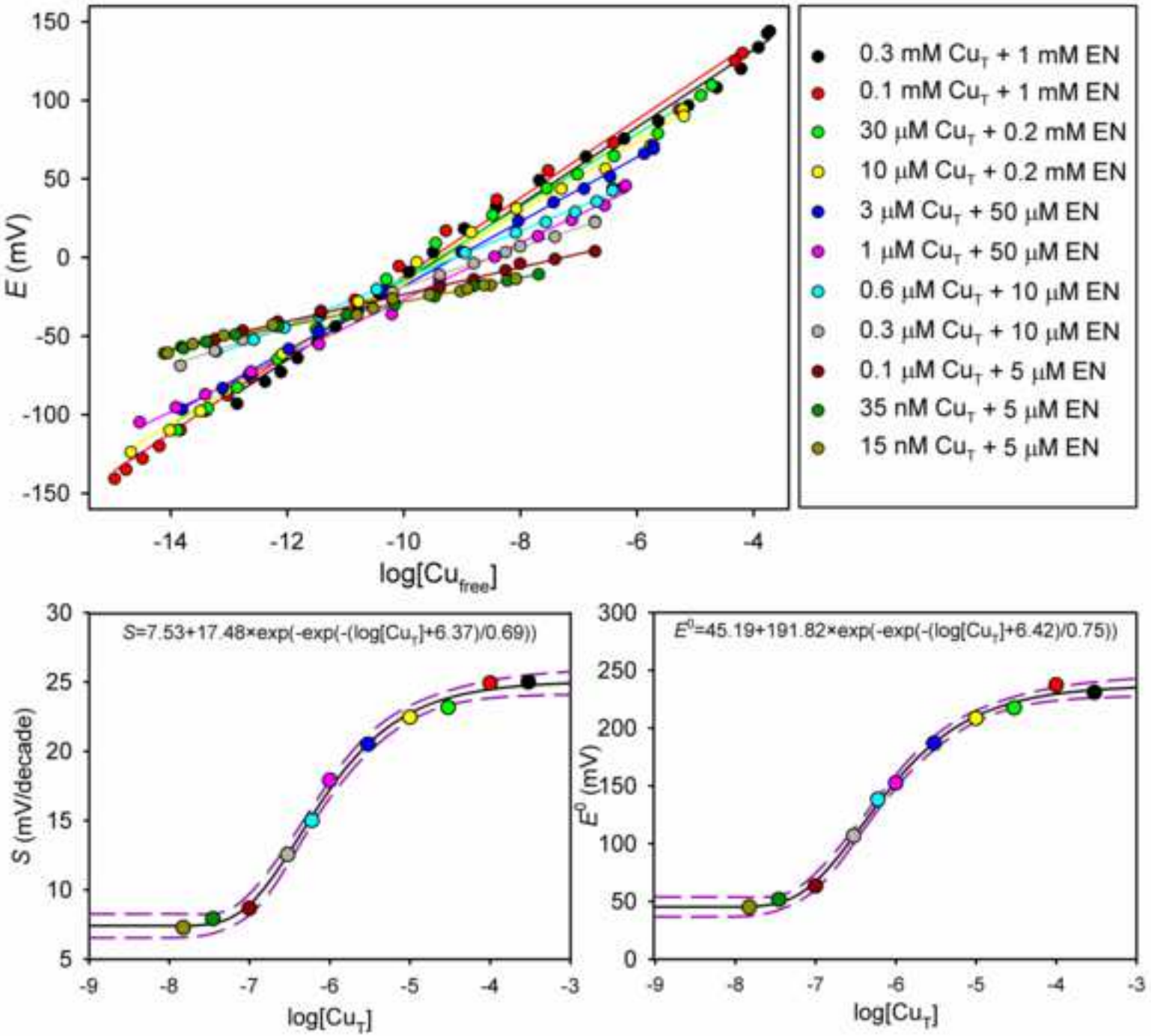

Figure 3

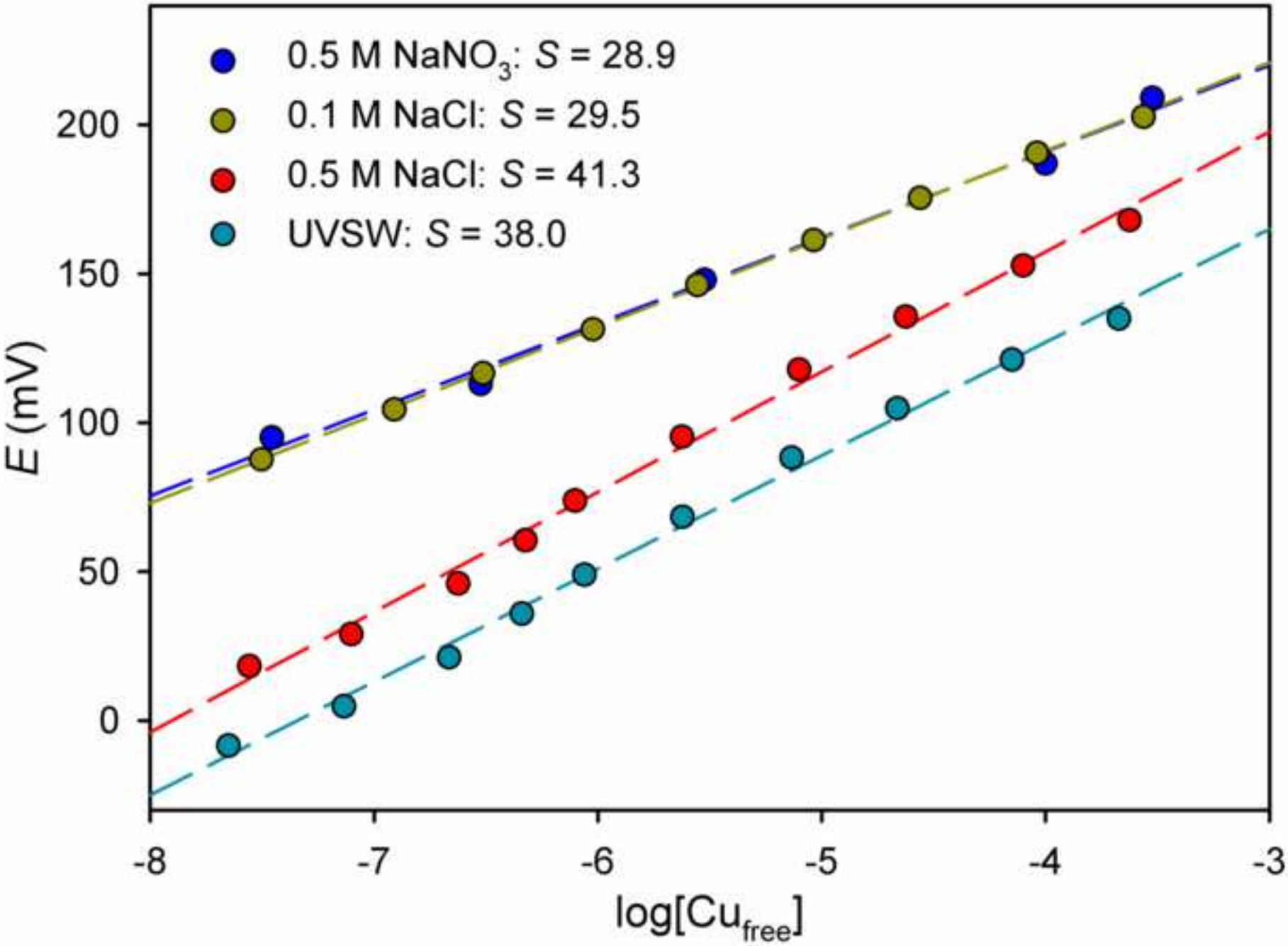

Figure 4

Click here to access/download;Figure;Figure_4.TIF

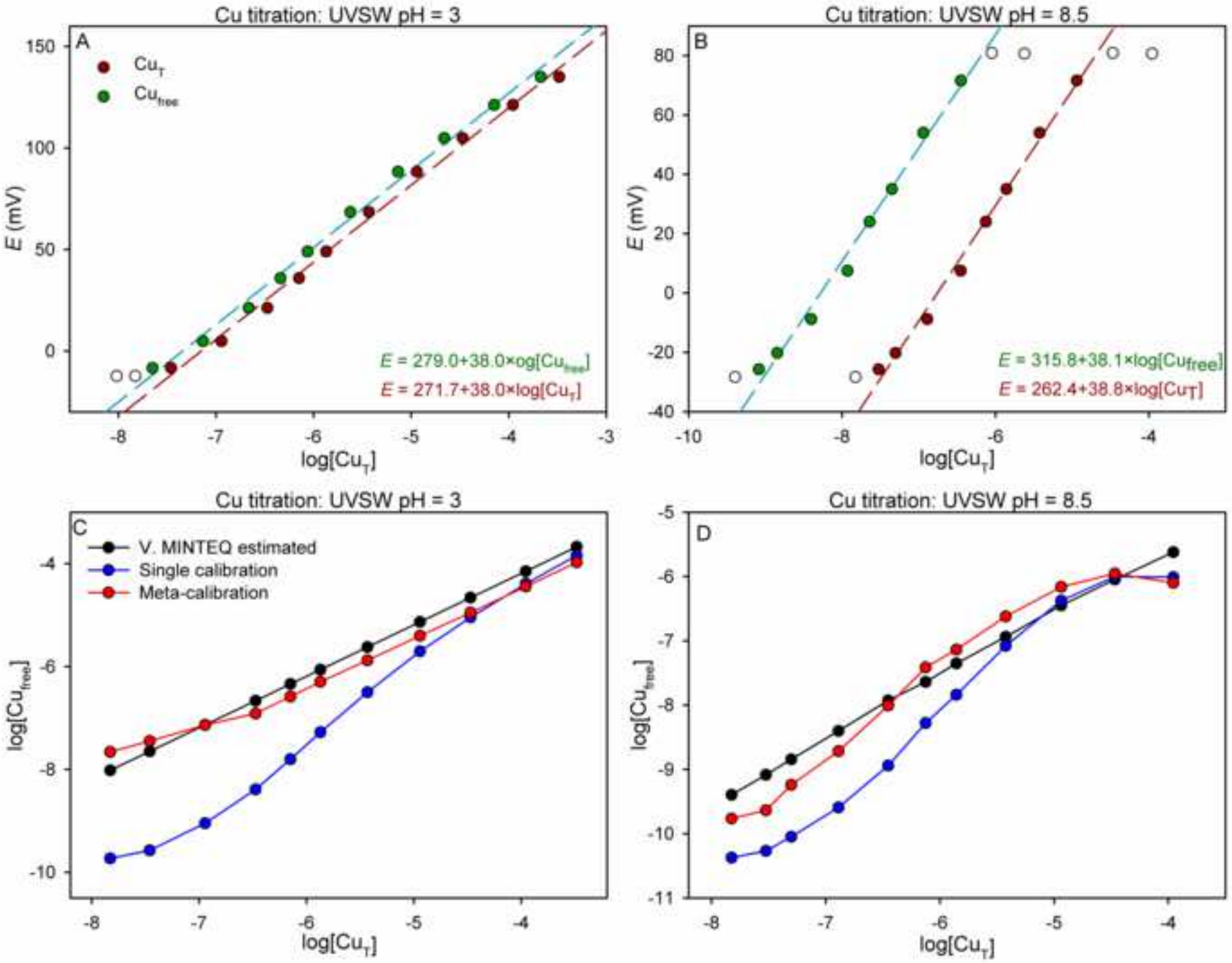

Figure 5

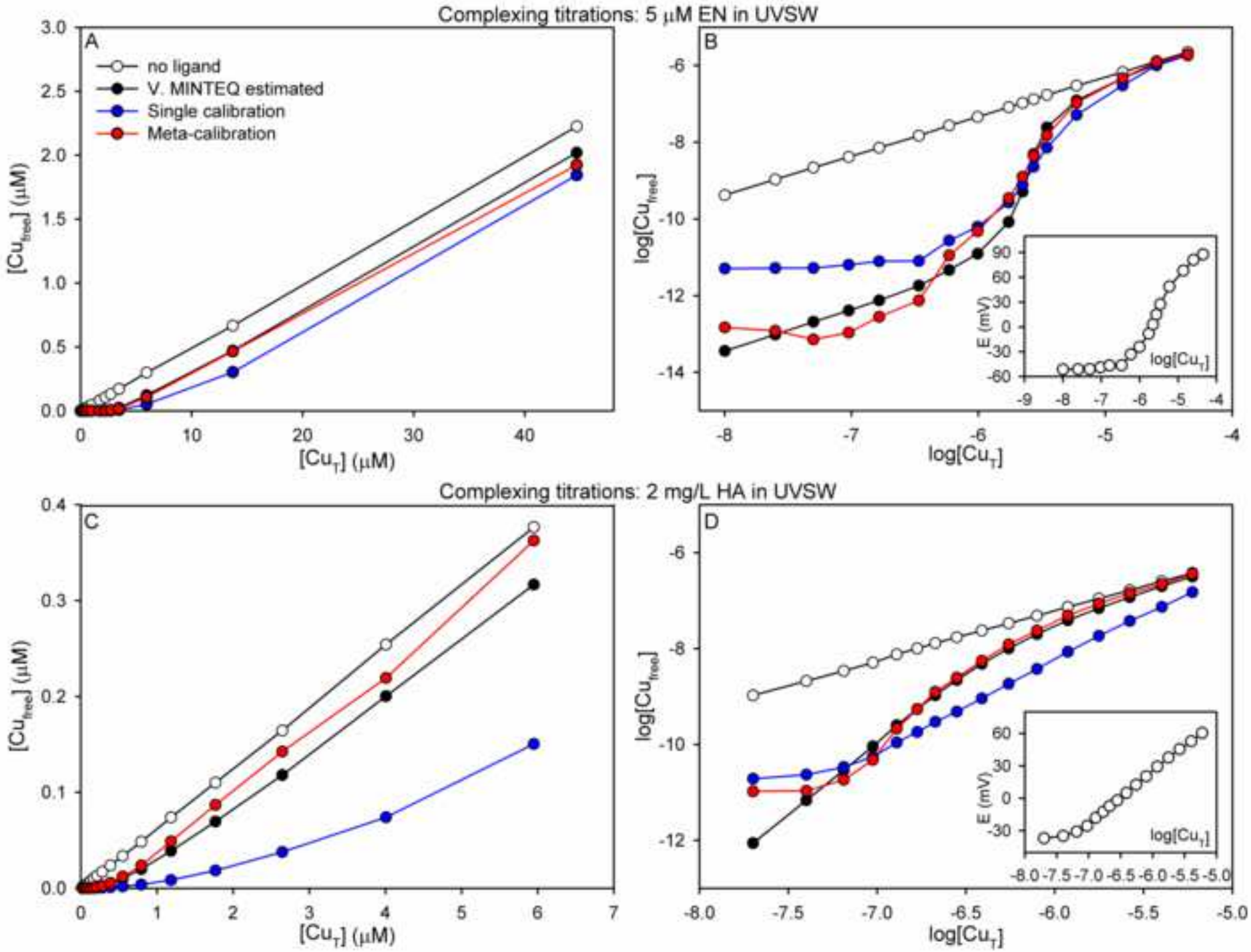

Figure 6

Click here to access/download;Figure;Figure_6.TIF

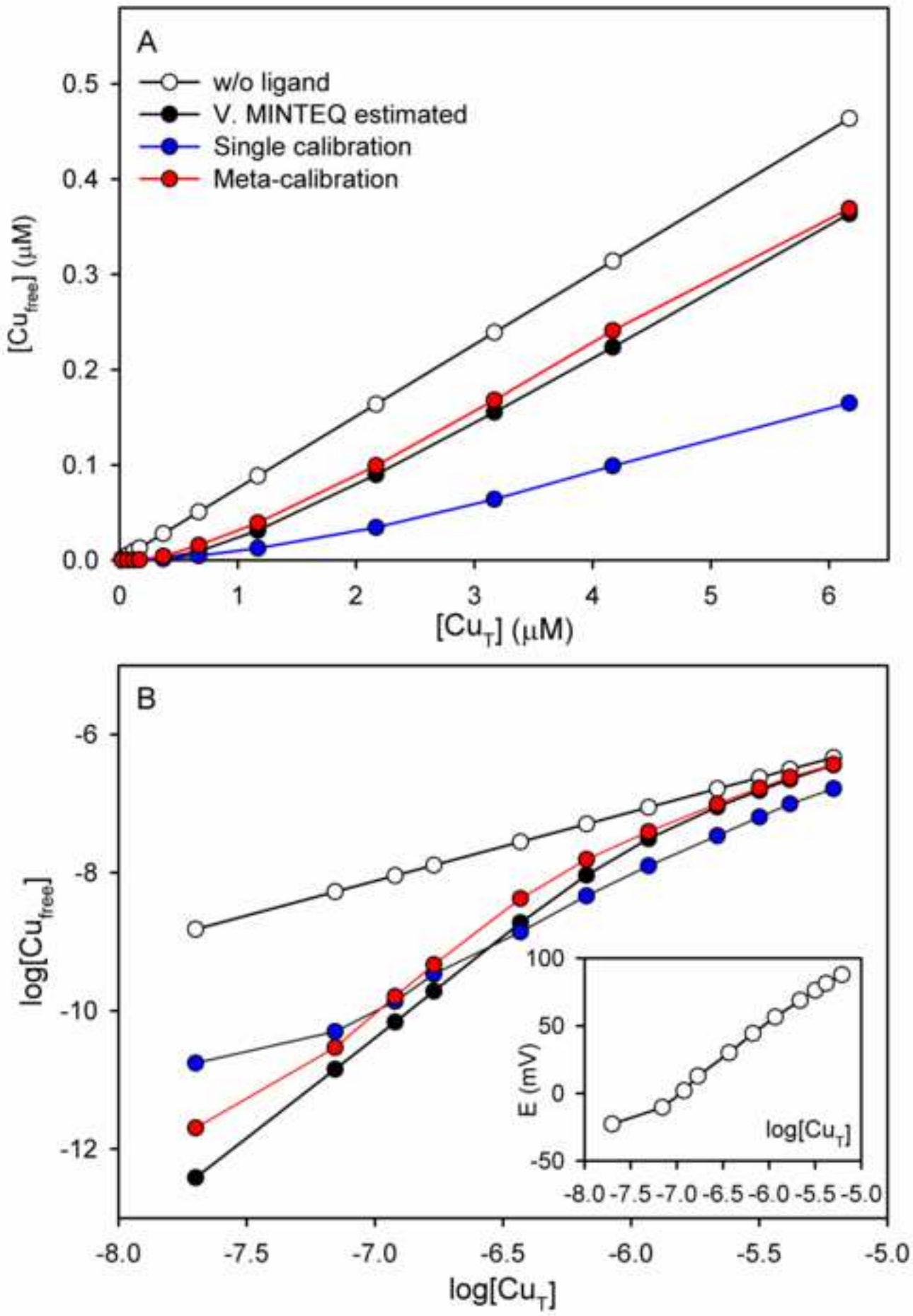

Figure 7

Click here to access/download;Figure;Figure_7.TIF